Supplemental Figures

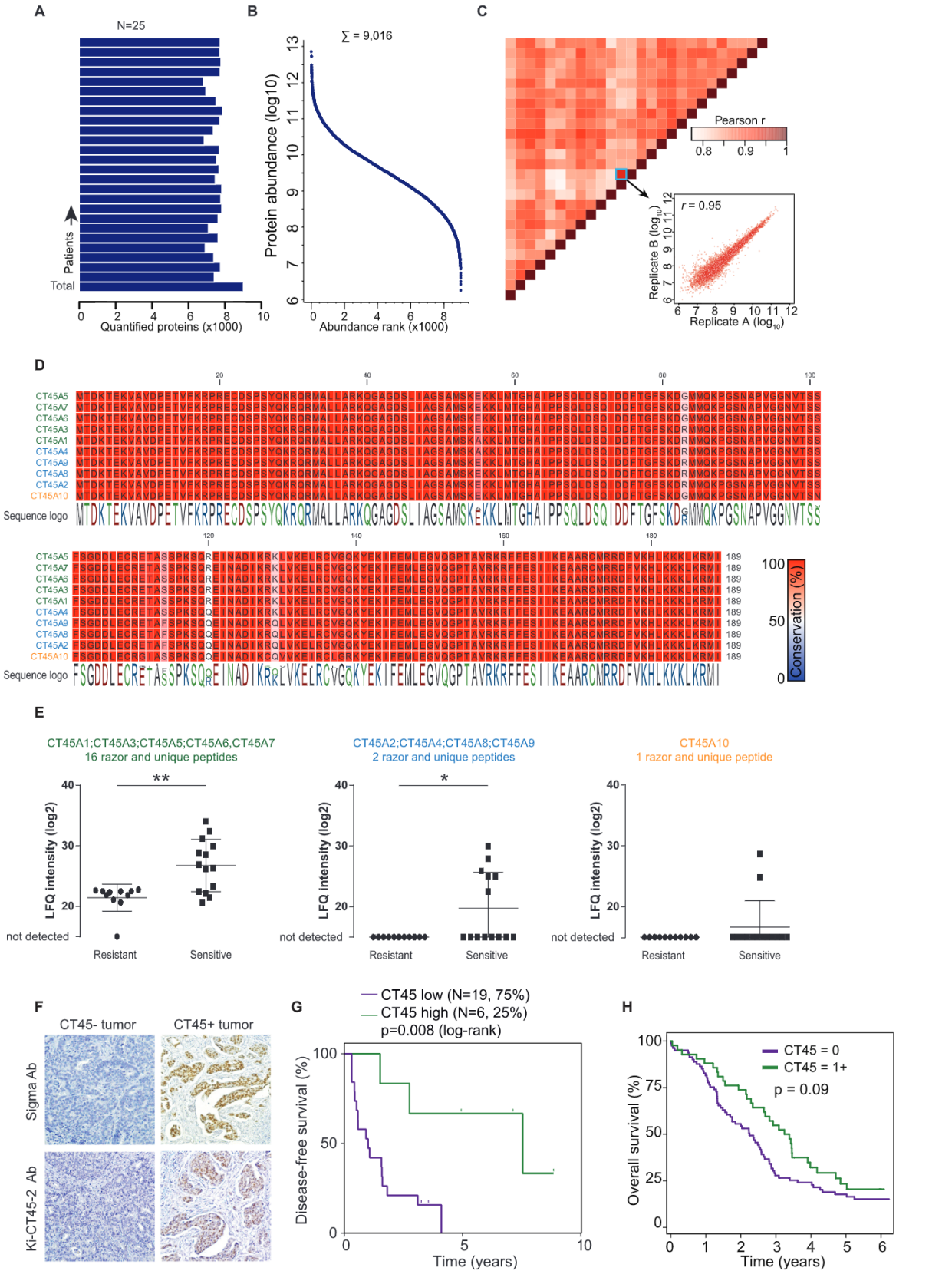

(legend on next page)

Figure S1. Discovery of CT45 by Shotgun Proteomics, Related to Figure 1

(A) Proteomic depth per patient. Samples were measured as technical duplicate.

(B) Dynamic range of protein abundance of all quantified proteins.

(C) Correlation matrix of all measured samples based on Pearson correlation values. The proteomic comparison of independently prepared tissue of the same tumor is highlighted (arrow).

(D) Amino acid alignment of the 10 members of the CT45 gene family. Color shows level of conservation with red being 100% and blue being 0%.

(E) Relative protein intensities (MaxLFQ, $\log_2$) for the three identified CT45 protein groups in chemosensitive and resistant patients. Note, the green CT45 protein group to which the majority of peptides was assigned (n = 16) is highlighted in Figure 1D. Error bars show standard deviation for each group. ** = p value < 0.01,* = p value < 0.05.

(F) Immunohistochemistry for CT45 based on two different antibodies (Sigma #SAB1301842 and Ki-CT45-2) in serial tumor sections from 2 representative patients.

(G) Kaplan-Meier survival analysis (log-rank test) for disease-free survival based on CT45 protein levels in the proteomics dataset. The patients with the highest CT45 expression (top 25%, n = 6, green, median disease-free survival = 90.5 months) are compared to the lower 75% (n = 19, purple, median disease-free survival = 12 months)

(H) Kaplan-Meier survival analysis (log-rank test) for overall survival based on CT45 staining scores from ovarian cancer TMAs. Advanced stage HGSOC patients comparing a staining score of 0 (n = 82) versus 1+ (n = 42) are compared.

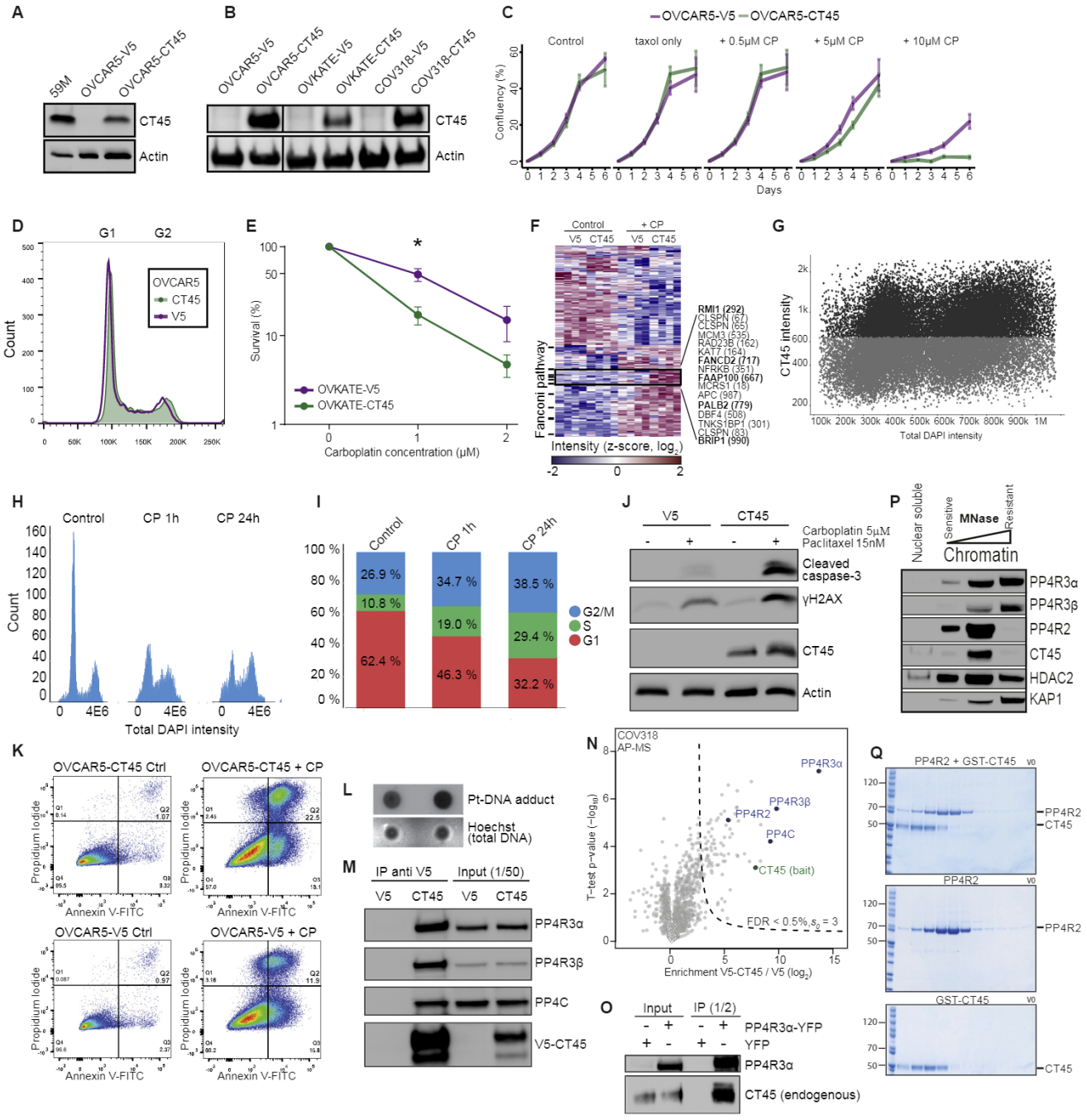

Figure S2. CT45 Sensitizes Cancer Cells to Carboplatin, Related to Figures 2 and 3

(A) Western blot of CT45 expression in OVCAR5 cells transduced with a pLX304-V5-CT45A5 lentivirus or control plasmid (pLX304-V5) compared to 59M cells with endogenous expression.

(B) Western blot of CT45 expression in ovarian cancer cell lines transduced with a pLX304-V5-CT45A5 lentivirus or control plasmid (pLX304-V5).

(C) Proliferation of OVCAR5 control (V5) or CT45 expressing cells with increasing concentrations of carboplatin. Error bars show standard deviation for each group.

(D) Cell cycle analysis of OVCAR5 control (V5) or CT45 expressing cells stained with propidium iodide.

(E) Clonogenic survival assay of the ovarian cancer cell line OVKATE stably overexpressing CT45 (green) or control (purple). Mean values are shown from three independent experiments. Error bars show SEM for each group. * = p value < 0.05.

(F) Phosphoproteomic analysis of the OVCAR-5 cell line pair ± 5 μM carboplatin treatment. Unsupervised hierarchical clustering of all ANOVA significant phosphorylation sites (FDR < 0.05, s_0 = 0.1) involved in DNA repair (GOBP) and DNA replication (GOBP) is plotted as heatmap. Proteins involved in the Fanconi anemia pathway are indicated by black lines. The phosphorylation site cluster specifically upregulated in CT45 expressing cells is highlighted in the black box.

(legend continued on next page)

(G) High-content immunofluorescence analysis of endogenous CT45 levels in 59M cells. Cells were co-stained with DAPI, CT45, and FANCD2 and gated according to high (black) or low (gray) CT45 expression. Gating strategy was applied for FANCD2 foci analysis in Figure 2C.
(H) Cell cycle profiles of untreated (control) and carboplatin treated (CP 1h and CP 24h) 59M cells based on total DAPI intensities from high-content immunofluorescence analysis.
(I) Proportions of cell cycle phases (G2/M, S and G1) of untreated (control) and carboplatin treated (CP 1h and CP 24h) 59M cells based on quantification of total DAPI and mean EdU intensities from high-content immunofluorescence analysis.
(J) Western blot of cleaved caspase-3, γH2AX, and CT45 following treatment of OVCAR-5 cells with carboplatin (5μM) and paclitaxel (1.5nM). Day 5.
(K) Flow cytometric analysis of CT45 expressing cells. OVCAR-5 cells stably expressing CT45 or a control vector (V5) were treated with 5 μM carboplatin for 72hr and then stained with Annexin-FITC and propidium iodide. Data is representative of 3 biological replicates.
(L) Dot blot for platinum-DNA adducts in the genomic DNA isolated from OVCAR5-V5 and OVCAR5-CT45 cells treated with carboplatin (day 3). Adducts were detected using an anti-cisplatin DNA adducts antibody. As a control for DNA loading, membranes were stained with Hoechst to visualize total DNA. Data is representative of 5 biological replicates.
(M) Western blot of immunoprecipitated V5-tagged CT45 protein in OVCAR-5 cells. The co-enriched members of the protein phosphatase 4 complex, PP4R3α, PP4R3β and PP4C, are shown.
(N) Interaction proteomics screen in the ovarian cancer cell line COV318 stably overexpressing V5-tagged CT45. Protein enrichment (t test difference) is calculated over the corresponding control cell line (V5 tag alone) and plotted against the t test p value ($-\log_{10}$). Dashed lines indicate significance thresholds ($p < 0.005$, $s_0 = 3$). The bait protein CT45 (green) and members of the protein phosphatase 4 complex (blue) are highlighted. Results represent 3 replicates per experiment group.
(O) Western blot of immunoprecipitated YFP-tagged PP4R3α protein in the 59M cell line endogenously expressing CT45. Immunoprecipitated YFP alone was used as control. The co-enriched CT45 is shown.
(P) CT45 positive 59M cells were collected and processed for a chromatin segregation assay as detailed in Material and Methods. PP4 complex members, KAP1, and HDAC2 were detected by western blot.
(Q) Gel filtration of recombinant PP4R2 and GST-CT45. PP4R2 and GST-CT45 were incubated for 10min on ice and loaded onto a Superdex 200 column (top panel) or run individually (middle panel: PP4R2, bottom panel: GST-CT45). Lanes represent serial elutions from the column.

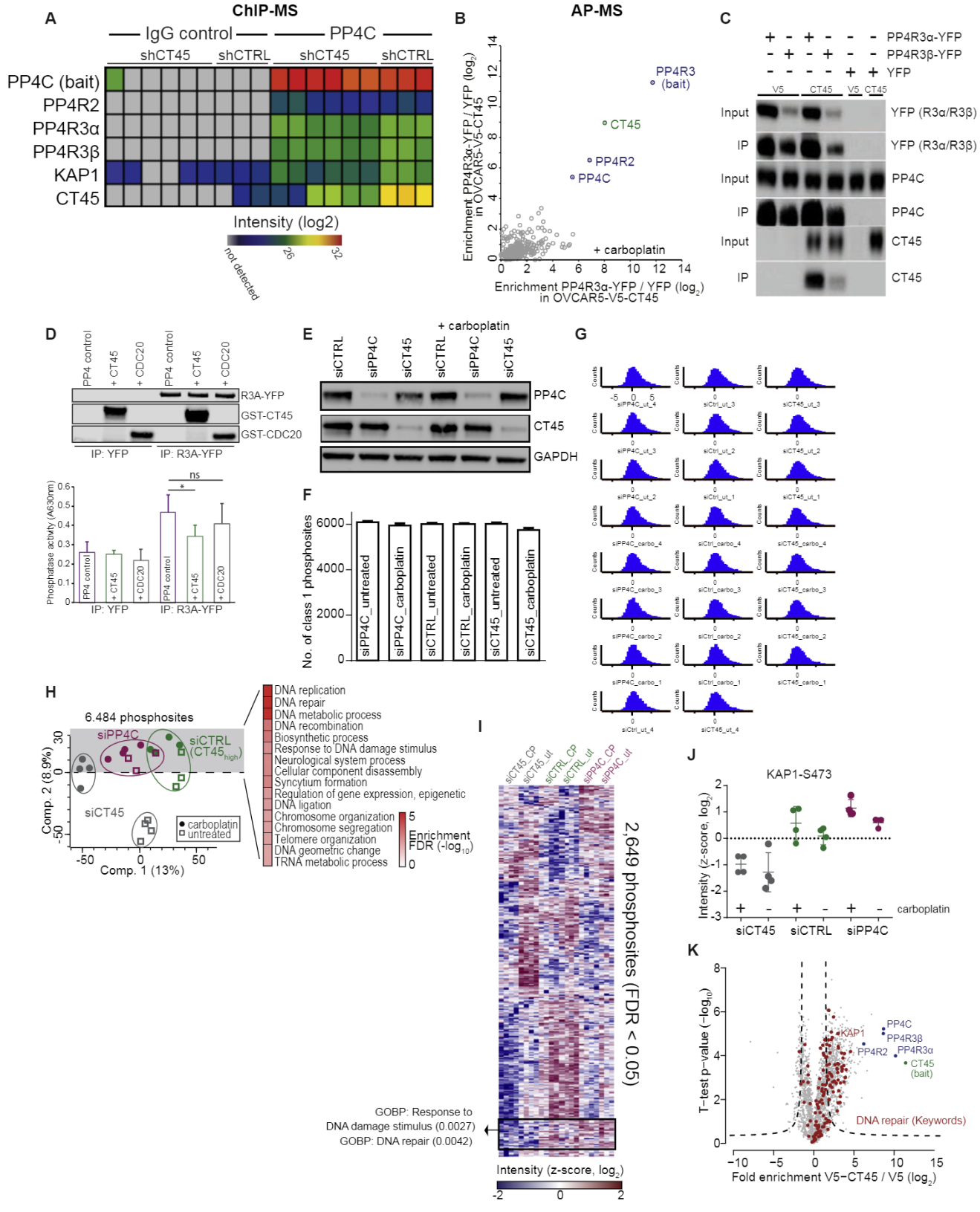

(legend on next page)

Figure S3. CT45 Is a PP4 Interactor Influencing DNA Damage Signaling, Related to Figure 3

(A) Chromatin-immunoprecipitation mass spectrometry (ChIP-MS) results for PP4C enriched chromatin in stable CT45 knock-down 59M cells versus 59M control cells. Heatmap shows MaxLFQ intensities (log_2) for the bait protein PP4C, the co-enriched PP4 complex members PP4R2, PP4R3α and PP4R3β, as well as CT45 and the known PP4 interactor KAP1. Results represent duplicate measurements of each of the three shRNA targeting CT45.

(B) Interaction proteomics screen in OVCAR5-V5-CT45 cells transiently overexpressing YFP-tagged PP4R3α or YFP alone ± 5 μM carboplatin treatment for 24h. Protein enrichment (t test difference) was calculated over the corresponding control cell line (YFP tag alone) for both conditions and plotted against each other. CT45 (green), as well as all detected PP4 complex members (blue) are highlighted.

(C) Western blot of the immunopurified PP4 complex using PP4R3α-YFP as bait protein in the presence or absence of CT45 in the OVCAR5 cell line pair. PP4C levels were used for normalization of the phosphatase assay in Figure 3F.

(D) Phosphatase activity assay of the immunopurified PP4 complex in the presence or absence of 3 μM recombinant GST-CT45 or GST-CDC20 control protein. Western blot (top panel) is shown as loading control. Quantification results (bottom panel) show raw values of the measured phosphatase activity (A630nm). Average values represent 5 independent experiments with a t test p value < 0.05. Error bars show standard deviation for each group.

(E) Western blot of 59M cells used for phosphoproteomic analysis. 59M cells were transfected with siRNAs against PP4C (siPP4C), CT45 (siCT45) or control (siCTRL), respectively.

(F) Number of class I phosphorylation sites identified in each sample group after data filtering (2 values in each group). Shown are average numbers for each of the 4 replicates. Error bars show standard deviation for each group.

(G) Intensity distribution (log_2) of all phosphorylation sites after data filtering.

(H) Phosphoproteomic analysis of CT45 (siCT45), PP4C (siPP4C) or control (siCRTL) siRNA knockdown 59M cells ± 4 μM carboplatin treatment for 72h. Left panel: Sample grouping based on principal component analysis of all phosphoproteomes, with component 1 accounting for 15% of total data variability and component 2 for 8.9%. Right panel: Pathway enrichment analysis of proteins with upregulated phosphosites along component 2. Significantly enriched terms are shown including Benjamini-Hochberg FDR values ($-log_{10}$).

(I) Unsupervised hierarchical clustering of all differentially regulated phosphorylation sites (FDR < 0.05, s_0 = 0.1) between PP4C, CT45 or control siRNA knockdown 59M cells after carboplatin (carbo) treatment or untreated (ut). Euclidean distances were used as distance measure for column and row wise clustering. The black box indicates a co-regulated cluster of the siPP4C and siCTRL group enriched for DNA damage repair pathways (GOBP). Numbers in brackets show Benjamini-Hochberg FDR values for pathway enrichment.

(J) Phosphorylation site intensity of the PP4 target site KAP1-S473. Shown are z-scored intensity values (log_2) for relative comparison across all samples. Error bars show standard deviation for each group.

(K) Volcano plot of chromatin-immunoprecipitation mass spectrometry (ChIP-MS) results for the V5-tag in OVCAR5-V5-CT45 versus OVCAR5-V5 cell line. Fold enrichment of V5-tagged CT45 over control cell line (V5 tag alone) is plotted against the t test p value ($-log_{10}$). Dashed lines indicate significance thresholds (FDR < 0.01, s_0 = 2). Proteins involved in DNA repair (Keywords) are highlighted in red.

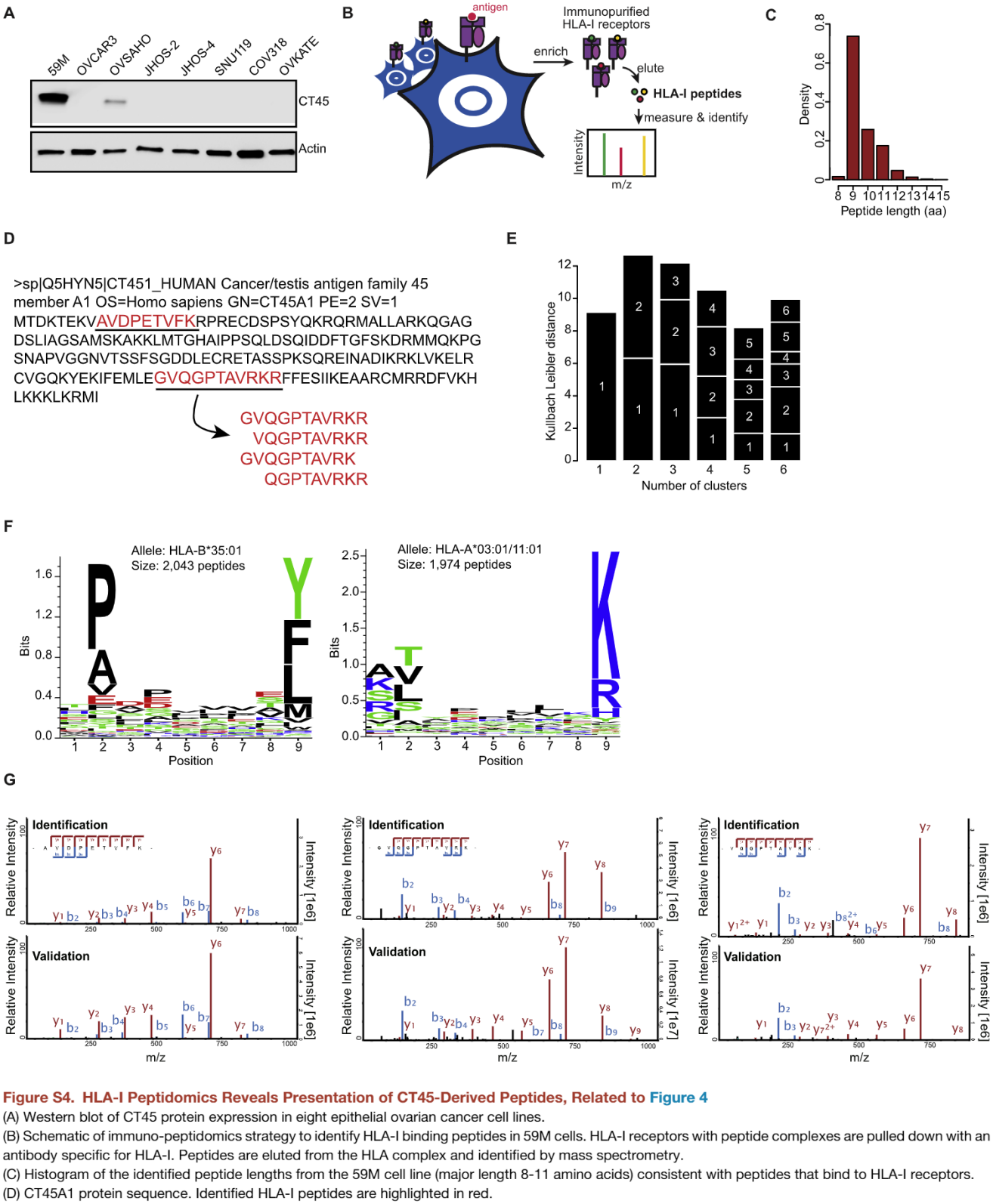

Figure S4. HLA-I Peptidomics Reveals Presentation of CT45-Derived Peptides, Related to Figure 4

(A) Western blot of CT45 protein expression in eight epithelial ovarian cancer cell lines.

(B) Schematic of immuno-peptidomics strategy to identify HLA-I binding peptides in 59M cells. HLA-I receptors with peptide complexes are pulled down with an antibody specific for HLA-I. Peptides are eluted from the HLA complex and identified by mass spectrometry.

(C) Histogram of the identified peptide lengths from the 59M cell line (major length 8-11 amino acids) consistent with peptides that bind to HLA-I receptors.

(D) CT45A1 protein sequence. Identified HLA-I peptides are highlighted in red.

(E) Identified consensus clusters based on the GibbsCluster −1.0 tool for all identified 9-mer peptides (4,017).

(F) Binding motifs. HLA-I consensus binding motifs for the two largest clusters in (E). The A11:01 motif is similar to A3:01.

(G) Comparison of MS/MS scans from experimentally identified HLA-I peptides (upper panel) and synthetic versions of the same peptides (lower panel). Y (red) and b-ions (blue) are shown.

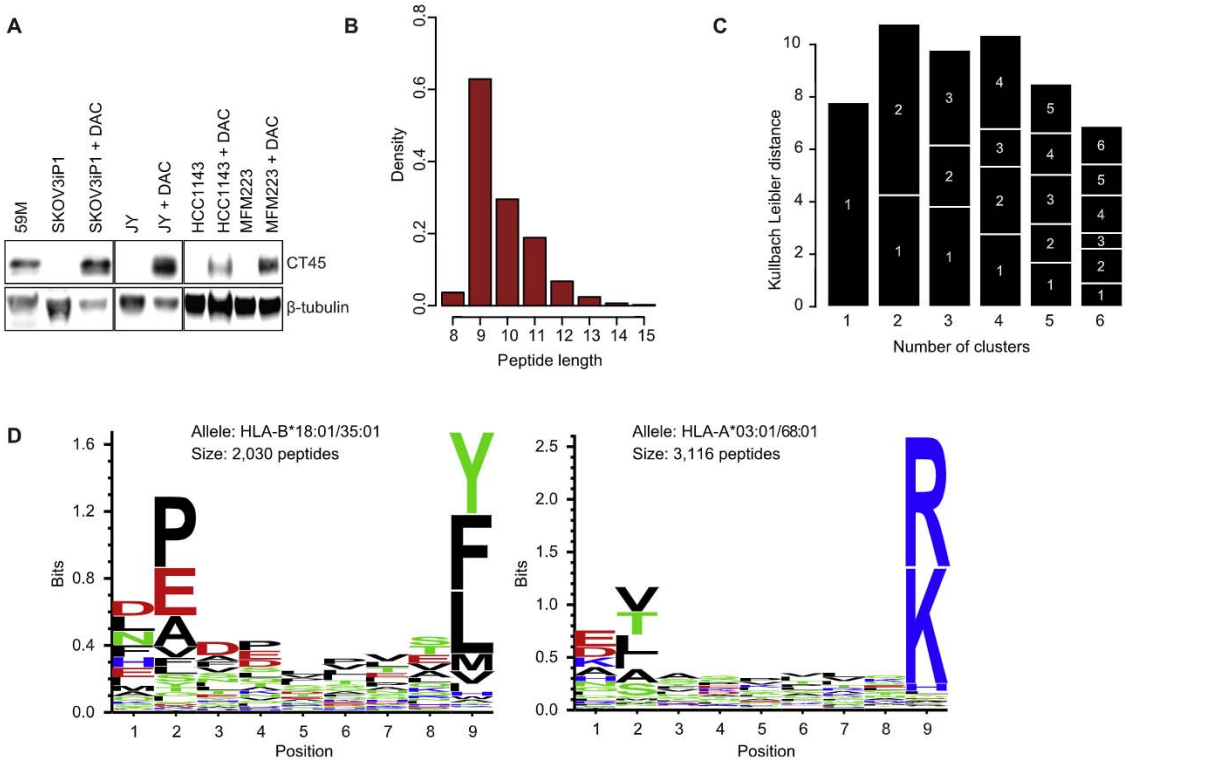

Figure S5. CT45-Derived Peptides Are Presented after DAC Treatment, Related to Figure 4

(A) Western blot of CT45 protein expression in SKOV3ip1 (HLA-A*03:01, 68:01), JY, HCC1143 and MFM223 cells following DAC treatment. 59M serves as positive control.

(B) Histogram of the identified peptide lengths from the DAC treated SKOV3ip1 cell line.

(C) Identified consensus clusters based on the GibbsCluster tool for all identified 9-mer peptides (5,146).

(D) HLA-I consensus binding motifs for the two largest clusters identified in (C). The A68:01 motif is similar to A3:01.